INTERNATIONAL JOURNAL OF HYDROGEN ENERGY XXX (2015) 1–11

Available online at www.sciencedirect.com

ScienceDirect

journal homepage: www.elsevier.com/locate/he

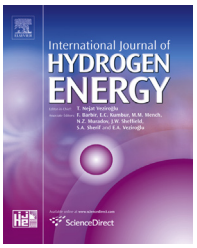

Production of hydrogen by catalytic steam reforming of oxygenated model compounds on Ni-modified supported catalysts. Simulation and experimental study

R. González-Gil [a], I. Chamorro-Burgos [a], C. Herrera [a,*], M.A. Larrubia [a], M. Laborde [b], F. Mariño [b], L.J. Alemany [a]

[a] Tecnologías de Procesos Catalíticos (PROCAT), Departamento de Ingeniería Química, Facultad de Ciencias, Universidad de Málaga, E-29071, Spain

[b] ITHES (CONICET/Universidad de Buenos Aires) – Pabellón de Industrias, Ciudad Universitaria, 1428, Argentina

ARTICLE INFO

Article history:
Received 19 January 2015
Received in revised form
12 May 2015
Accepted 26 May 2015
Available online xxx

Keywords:
Hydrogen
Oxygenated compounds
Steam reforming
Ni-modified catalysts
Mathematical model

ABSTRACT

Steam reforming of two representative components in the aqueous fraction of bio-oil, acetone and ethanol, was investigated over nickel based supported catalysts (Ni/Al_2O_3). The effect of Rh incorporation ($Ni–Rh/Al_2O_3$) and the properties of different γ-Al_2O_3 used as support was tested. Hydrogen-rich gas is produced at temperatures higher than 673 K in both acetone and ethanol reforming with maximum mole fraction of 0.6–0.7. The reactions involved and the possible routes were studied. Rh incorporation and nanostructured alumina affects the Ni metal size and the amount of carbon deposited onto catalysts' surface after reforming tests; besides, acetone is also found as an important intermediate in ethanol reforming, and Rh improve hydrogen production with negligible intermediates presence. The effect of S/Acetone or S/Ethanol feed molar ratios, space velocity and temperature over acetone/ethanol conversion and over H_2/CO ratio were modeled using the Matlab software in order to find the regions and the optimal operating conditions in both processes. Simulation results are consistent with the experimental data.

Introduction

Development of clean, sustainable, and cost-competitive hydrogen production processes is essential to the market success of hydrogen-powered vehicles and fuel cells. Hydrogen is recognized as an important energy carrier and plays an important role in the future global economy [1,2]. The perspective of using hydrogen as a fuel in the future depends to a great extent on finding alternatives to the existing production technologies and feedstock. Most efforts are being dedicated to develop the utilization of renewable energy sources. Most hydrogen is currently produced from fossil fuels such as natural gas, naphtha and coal, and the traditional processes for hydrogen production are the catalytic steam reforming followed by water gas shift conversion [3–9].

* *Corresponding author*. Tel.: +34 952131914.
E-mail address: concepcionhd@uma.es (C. Herrera).

http://dx.doi.org/10.1016/j.ijhydene.2015.05.167

However, one of the limitations of current hydrogen generation is the depletion of these sources and the substantial amounts of CO_2 emitted to the atmosphere during the process steps associated with this production. Biomass is an abundant and carbon-neutral renewable energy resource for the production of alternative liquid fuels and a variety of chemicals. Much experimental and modeling works have been performed to date on converting biomass to hydrogen using different thermochemical pathways, mostly involving gasification or pyrolysis of biomass at various temperatures and pressures [10–14]. Fast pyrolysis for liquids production is currently of particular interest as the liquid can be stored and transported, and used for energy, chemicals or as an energy carrier. Recent developments in flash pyrolysis technologies make possible to convert biomass efficiently to a bio-oil, a mixture of oxygenated compounds including acids, alcohols, ketones, esters, ethers, aldehydes, phenols, and its derivatives, as well as carbohydrates, and a large proportion of lignin-derived oligomers. Steam reforming of aqueous bio-oil fractions is therefore an interesting alternative to produce hydrogen in a renewable way. Due to the complexity of steam reforming of bio-oils, it is useful to study the individual reforming behavior of the different chemical families in bio-oil, where alcohols, acids and ketones are the three major chemicals families [15]. Reforming of model-oxygenated components have been studied in last decades [16–19], most of the studies reported in literature have been focused on the reforming of acetic acid [20–24]. Whereas acetone steam reforming has been less studied, ethanol steam reforming have been extensively studied [25–27]. On the other hand, acetone-reforming study is interesting in the key of acetone is an important intermediate during reforming of ethanol.

According to literature, different supported catalysts have been used in steam reforming of oxygenated compound: Ni–Zn–Al [28], Ni/ZrO_2 [29], $Co–Ce/Al_2O_3$, $Co–La/Al_2O_3$ [30], Pt/ZrO_2 and Pt/CeO_2 [31] and lanthanum oxide or La_2O_3 modified alumina [32], metal which is used to prevent thermal sintering of alumina [33]. Ni-based catalysts have been widely used for reforming of bio-oil, due to the high C–C bond-breaking activity and the relatively low cost. However, Ni/Al_2O_3 catalyst is subject to coking, which leads to its fast deactivation during steam reforming. Rh-based catalyst reported high reforming capabilities and, all metals in general show higher selectivity towards CO_2 indicating some ability to promote water gas shift and other reactions [34,35], Rh is also able to reform ethylene with ease what implies a reduction in carbon deposition. The nature of support also plays an important role towards product selectivity and the deactivation behavior of the catalyst. Acidic supports like Al_2O_3 are more prone to deactivation on account of coke formation.

In the present study, Ni-based Al_2O_3 supported catalysts were prepared and tested for hydrogen production via steam reforming of acetone (SRA) and ethanol (SRE). Acetone and ethanol were selected as model compounds for the various carbonyl-containing (mainly aldehydes and ketones) and alcohols (phenols) constituents of the aqueous fraction of bio-oil (from biomass fast pyrolysis). The influence of the incorporation of small amount of Rh to the Ni/Al_2O_3 and the properties of different γ-Al_2O_3 used as support was also investigated. Furthermore a mathematical model was developed to simulate the processes and predict the best operating condition to obtain a H_2-rich stream.

Experimental

Catalyst preparation and characterization

Heterogeneous catalysts were prepared by incipient wetness impregnation method using a commercial γ-Al_2O_3 Puralox TH 100/150 from Sasol ($A_{BET} = 144\ m^2\ g^{-1}$and $V_p = 0.97\ cm^3\ g^{-1}$) denoted as Al_2O_3 (TH) and a synthesized nanofibrous gamma alumina ($A_{BET} = 300\ m^2\ g^{-1}$and $V_p = 0.70\ cm^3\ g^{-1}$), denoted as Al_2O_3 (N) as supports. Al_2O_3 (N) was prepared from $NaAl_2O_3$ with a non-ionic surfactant (Tergitol 15-TS-5, Sigma) in ratio of Tergitol/Al = 0.5 to control the fibers, size and morphology [36,9]. $Ni(NO_3)\cdot 6H_2O$ and $Rh(NO_3)_3\cdot x(H_2O)$ were used as Ni and Rh precursors respectively for all catalysts. Monometallic Ni (9 at nm^{-2}; labeled as Ni/Al_2O_3(TH) or Ni/Al_2O_3(N)) catalysts were prepared, as well as a bimetallic $Ni–Rh/Al_2O_3$ using the minimum Rh content, in atomic ratio 1:100 respect to Ni loaded (9 at nm^{-2} of Ni and 0.09 at nm^{-2} of Rh; labeled as Rh–Ni/Al_2O_3(TH)). After impregnation, catalysts were dried at room temperature for 24 h, and calcined at 873 K for 2 h. A deep characterization study of the fresh catalysts as well as of the gamma alumina used as support can be found in our previous studies [9,37].

Catalysts were characterized after 10 h of reaction by different methods. XRD data have been recorded with an X'Pert MPD PRO diffractometer (PANalytical) using CuKα1 radiation and a Ge (111) primary monochromator. The amount of carbon deposited on catalyst surface after 10 h of reaction was analyzed by elemental analysis (CNHSO) using an Elemental Analyzer Perkin–Elmer 2400 CHN and by Raman spectroscopy. Raman spectra were collected in a DXR Raman Microscope (Thermo Scientific) working at $\lambda = 532$ nm and 10 mW and incorporating a CCD detector.

Catalytic activity

The experiments were performed at atmospheric pressure in a Micro Activity PID Eng&Tech system consisting of a fixed-bed flow reactor (i.d. 9 mm) and a mass flow controller unit. An HPLC pump (Gilson 307) was used for feeding the liquid reactants (a mixture of acetone or ethanol and water) to the reactor. The fixed bed reactor was equipped with a coaxial thermocouple placed at the center of catalyst bed to monitor the reactor temperature. Separation and quantification of the gas products were attained by on-line gas chromatograph (Agilent 7820A GC) equipped with thermal-conductivity detector (TCD) and flame ionization detector (FID).

A temperature range from 473 to 973 K at atmospheric pressure was used, with a steam to carbon molar ratio (S/C) equal to 3 in case of acetone [38] and S/C equal to 2 for ethanol reforming [39]. The inlet flow of the acetone/ethanol–water mixture was set at 0'9 Ncm^3h^{-1} (0.004 $mol_{acetone}h^{-1}$ and 0.007 $mol_{ethanol}h^{-1}$) with a helium flow of 30 Ncm^3min^{-1} as diluent. The catalyst (0.1 g, 250–420 μm) diluted with an equal amount of quartz was placed in the reactor working at

Please cite this article in press as: González-Gil R, et al., Production of hydrogen by catalytic steam reforming of oxygenated model compounds on Ni-modified supported catalysts. Simulation and experimental study, International Journal of Hydrogen Energy (2015), http://dx.doi.org/10.1016/j.ijhydene.2015.05.167

9000 h^{-1}, operating under plug flow conditions. Previous tests with different catalyst particle sizes and dilutions were performed to confirm the non-existence of heat or mass transfer limitations. Before the reaction, the catalysts were reduced in situ in H_2-atmosphere (20% H_2–He, 0.5 Ncm^3s^{-1}) during 2 h at 873 K. Results are reported based on the oxygenated-compound conversion, products mole fraction and H_2/CO and H_2/CO_2 molar ratios, on dry basis. C, H and O balances were closed with deviations lower than 5%.

Reaction network analysis

Steam reforming of model components with chemical formula of $C_nH_mO_k$ can be described by Eq. (1). The yield is also influenced by the Water Gas Shift reaction, WGS, (Eq. (2)) depending on the conditions of the reactions. The overall reforming reaction can be represented as Eq. (3), and, for acetone and ethanol, according to Eqs. (4) and (5) respectively, although at high temperatures the WGS is shifted to the left and CO will be also present in significant amounts.

$$C_nH_mO_k + (n-k)\,H_2O \rightarrow n\,CO + (n+(m/2) - k)\,H_2 \quad (1)$$

$$CO + H_2O \leftrightarrow CO_2 + H_2 \quad (2)$$

$$C_nH_mO_k + (2n - k)\,H_2O \rightarrow n\,CO_2 + (2n + (m/2) - k)\,H_2 \quad (3)$$

$$C_3H_6O + 5H_2O \rightarrow 3CO_2 + 8H_2 \quad (4)$$

$$C_2H_5OH + 3H_2O \rightarrow 6H_2 + 2CO_2 \quad (5)$$

Thermal decomposition for most oxygenates can occur forming mainly coke and a mixture of gases as presented in Eq. (6). Moreover, acetone decomposes according to an endothermic reaction into ketene and methane (Eq. (7)), at temperatures above 773 K, according to literature and unpublished previous results [40–44]. Furthermore, under these conditions, ketene decomposition or ketene coupling can occur as a parallel process with ethylene and CO as principal products (Eq. (8)).

$$C_nH_mO_k \rightarrow C_xH_yO_z + \text{gas } (H_2, CO, CO_2, CH_4 \ldots) + \text{coke} \quad (6)$$

$$CH_3COCH_3 \rightarrow CH_2CO + CH_4 \quad (7)$$

$$CH_2CO \rightarrow 1/2C_2H_4 + CO \quad (8)$$

Additionally, ketene may be converted to acetic acid via hydration (Eq. (9)) and, via Eq. (10), ketene hydration can also contribute but to a lesser extent to the formation of methane and carbon dioxide. Carbon monoxide and acetic acid may also arise from the alternative reforming of acetone via reaction in Eq. (11). Steam reforming of ketene (Eq. (12)) also contribute to increase H_2 content.

$$CH_2CO + H_2O \rightarrow CH_3COOH \quad (9)$$

$$CH_2CO + H_2O \rightarrow CH_4 + CO_2 \quad (10)$$

$$CH_3COCH_3 + 2H_2O \rightarrow CH_3COOH + CO + 3H_2 \quad (11)$$

$$CH_2CO + H_2O \leftrightarrow 2CO + 2H_2 \quad (12)$$

For ethanol reforming, an alternative reaction can occur, with insufficient steam supply, as presented in Eq. (13). Depending on the acidity of the catalyst, two major undesirable routes should be also included, dehydrogenation to form acetaldehyde (Eq. (14)) which, in the current reaction conditions can be reformed too (Eq. (15)), and dehydration to ethylene (Eq. (16)), the main source of coke formation. Ethanol decomposition pathways can also contribute to final products, as shown in Eq. (17) and Eq. (18), with methane formation, which can be also reformed (Eq. (19)); and acetone [45–50], which can undergo the network proposed above. In both cases, SRA and SRE, methane formed can be reformed according to Eqs. (19) and (20) under these conditions. As it can be seen, the hydrogen production varies significantly with the different reactions network.

$$C_2H_5OH + H_2O \rightarrow 4H_2 + 2CO \quad (13)$$

$$C_2H_5OH \rightarrow C_2H_4O + H_2 \quad (14)$$

$$C_2H_4O + H_2O \rightarrow 2CO + 3H_2 \quad (15)$$

$$C_2H_5OH \rightarrow C_2H_4 + H_2O \quad (16)$$

$$C_2H_5OH \rightarrow CH_4 + CO + H_2 \quad (17)$$

$$2C_2H_5OH \rightarrow C_3H_6O + CO + H_2 \quad (18)$$

$$CH_4 + H_2O \rightarrow CO + H_2O \quad (19)$$

$$CH_4 + 2H_2O \rightarrow CO_2 + 4H_2 \quad (20)$$

Mathematical model

Reactions, kinetics and thermodynamics parameters for mathematical model are listed in Table 1 [41,44,51]. Based on

Please cite this article in press as: González-Gil R, et al., Production of hydrogen by catalytic steam reforming of oxygenated model compounds on Ni-modified supported catalysts. Simulation and experimental study, International Journal of Hydrogen Energy (2015), http://dx.doi.org/10.1016/j.ijhydene.2015.05.167

Table 1 – Reactions set and some kinetics parameters used in the mathematical model for the simulation of acetone and ethanol steam reforming.

	ΔH^0_{298K} (KJmol^{-1})	k_o (mols^{-1}kgcat^{-1} atm^{-n})	$-\Delta G^0_{298K}$ (KJmol^{-1})	Ea (kJmol^{-1})	Reaction kinetic
Steam reforming of acetone					
Eq. (4)	246.30	$5.10\cdot10^{-3}$	112.78	195.55	$r_1 = k_1 \cdot \left(p_{CH_3COCH_3} - \frac{p^3_{CO_2}\cdot p^8_{H_2}}{K_{1eq}\cdot p^5_{H_2O}}\right)\cdot P^{-0.5}$
Eq. (7)	80.77	$1.93\cdot10^{6}$	44.32	374.11	$r_2 = k_2 \cdot \left(p_{CH_3COCH_3} - \frac{p_{CH_4}\cdot p_{CH_2CO}}{K_{2eq}}\right)\cdot P^{-0.5}$
Eq. (19)	206.00	$8.95\cdot10^{9}$	141.86	154.00	$r_3 = k_3 \cdot \left(p_{CH_4} - \frac{p_{CO}\cdot p^3_{H_2}}{K_{3eq}\cdot p_{H_2O}}\right)\cdot P^{-0.5}$
Eq. (2)	−41.00	$6.08\cdot10^{6}$	−28.67	70.00	$r_4 = k_4 \cdot \left(p_{CO} - \frac{p_{H_2}\cdot p_{CO_2}}{K_{4eq}\cdot p_{H_2O}}\right)\cdot P^{-0.5}$
Eq. (8)	80.00	$1.00\cdot10^{6}$	−42.64	274.21	$r_5 = k_5 \cdot \left(p_{CH_2CO} - \frac{p^{0.5}_{C_2H_4}\cdot p_{CO}}{K_{5eq}}\right)\cdot P^{-0.5}$
Steam reforming of ethanol[a]					
Eq. (17)	49.00	$7.26\cdot10^{5}$	–	87.00	$r_1 = k_1 \cdot p_{C_2H_5OH}$
Eq. (20)	165.10	$8.78\cdot10^{10}$	113.59	156.00	$r_2 = k_2 \cdot \left(p_{CH_4}\cdot P^2_{H_2O} - \left(\frac{p_{CO_2}\cdot p^4_{H_2}}{K_2}\right)\right)$

[a] Eqs. (19) and (2) and their kinetic parameters are also considered in ethanol steam reforming.

our experimental results, five majors reactions, namely acetone reforming (Eq. (4)), acetone decomposition (Eq. (7)), methane reforming (Eq. (19)), Water Gas Shift (Eq. (2)) and ketene decomposition (Eq. (8)), are considered for acetone steam reforming, where hydrogen, carbon monoxide, carbon dioxide, methane, ketene, ethylene and water were considered as the products for the simulation model. In ethanol reforming process, ethanol decomposition (Eq. (17)), methane steam reforming (Eqs. (19) and (20)) and WGS are considered, being hydrogen, carbon monoxide, carbon dioxide and methane the products considered in the mathematical model. The reaction system is an isothermal and one-dimensional fixed-bed reactor in which catalysts are packed. In order to represent the steady-state operation of the steam reforming, a pseudo-homogeneous model was adopted to develop the mathematical model subject to the assumption that the process occurs without axial dispersion. A Matlab subroutine function was used to numerical integrate the differential equations, mass balance of each component, Eq. (21) and energy balance Eq. (22), along the length of the reactor, thus determining the temperature and concentration profiles.

$$dF_i/dz = f(r_i,\ T) \tag{21}$$

$$\frac{dT}{dz} = \frac{\left(\frac{4\cdot U}{\rho_B\cdot D}\right)(T_f - T) + \left(-\sum \Delta H_{r_i}\cdot r_i\right)}{\sum F_i\cdot Cp_i}\cdot \rho_B\cdot A \tag{22}$$

$$\sum \Delta H_{r_i}(T) = \left(\Delta H^0_{r_i}(T_R)\right) + \Delta Cp(T - T_R)$$

ΔH_{r_i} (i = 1–5 or 1–4) corresponds to the enthalpy of each reaction. The calorific capacities (ΔCp) are appraised for polynomial expressions in function of the temperature.

Considered all boundary conditions are given at z = 0, therefore, the set of ODEs constitutes the initial value problem. In present study, the set of ODEs is solved by using ODE solver "ode45" and "ode15s" in Matlab, depending on the problem stiffness. The performance has been analyzed in terms of conversion of acetone or ethanol and H_2/CO molar ratios.

Results and discussion

Characterization

Fig. 1 shows the XRD pattern of the catalysts after SRA and SRE. All diffractograms present the characteristic lines of pseudo-amorphous gamma Al_2O_3 (JCPDS 75-0921), which were slightly shifted to lower Bragg's angle due to the presence of $NiAl_2O_4$ (JCPDS 01-1299). Besides, metallic Ni (JCPDS 89-8489) was also registered. Strong signals that can be observed in some of the diffractograms correspond to quartz (JCPDS 01-070-3755) used as a catalysts diluent in the experiments, been,

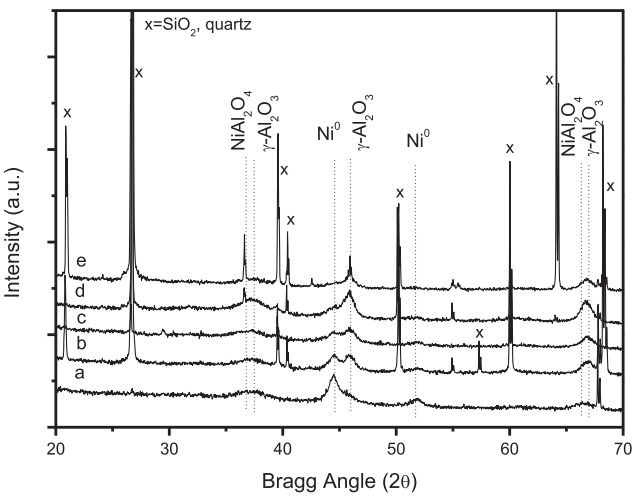

Fig. 1 – XRD patterns of the catalysts after reaction. (a) Ni/Al_2O_3(TH) after SRA; (b) Ni–Rh/Al_2O_3(TH) after SRA; (c) Ni/Al_2O_3(TH) after SRE; (d) Ni–Rh/Al_2O_3(TH) after SRE and (e) Ni/Al_2O_3(N) after SRE.

Please cite this article in press as: González-Gil R, et al., Production of hydrogen by catalytic steam reforming of oxygenated model compounds on Ni-modified supported catalysts. Simulation and experimental study, International Journal of Hydrogen Energy (2015), http://dx.doi.org/10.1016/j.ijhydene.2015.05.167

Table 2 – Average particle size of Ni^0, carbon content and carbon graphitic fraction of the catalysts after SRA and SRE reactions.

Catalyst	D_pNi^0 (nm)[a]		C (wt%)[b]		X_G[c]	
	SRA	SRE	SRA	SRE	SRA	SRE
Ni/Al_2O_3 (TH)	9	20	2	17.2	0.31	0.42
$Ni–Rh/Al_2O_3$ (TH)	n.d.	13	1	5.8	0.38	0.30
Ni/Al_2O_3 (N)	–	n.d.	–	2.7	–	0.36

n.d. means not determined.
[a] Average particle size of Ni^0, calculated by the Scherrer equation.
[b] Carbon content of the catalysts after ASR and ESR reactions, obtained by elemental analysis.
[c] Carbon graphitic fraction calculated from D and G Raman signals after ASR and ESR reactions.

in some cases very difficult to separate from it. Average particle size of Ni^0 was calculated by the Scherrer equation, the results obtained are summarized in Table 2. It is worth notice that the Ni^0 size is lower than 20 nm for all systems and that, as was reported before [9], the incorporation of Rh, even in very low concentration (Ni:Rh = 100:1, in atomic ratio), and the alumina support affect the Ni^0 metal size. No graphitic carbon signals were detected by XRD. Carbon content (wt%) on catalysts after reaction was studied and the results are presented in Table 2. For SRA, the amount of carbon deposited is very low compared to the obtained for SRE. Moreover, it can be deduced that, as well as the D_pNi^0, the carbon content seems to be dependent not only on the Rh incorporated but also on the properties of the alumina support. When Rh is added to Ni/Al_2O_3 (TH) catalyst, the amount of carbon measured decrease, Rh promotes the carbon gasification aided by the steam in the feed and the support effect can be explained also with regard to the acidity. Al_2O_3 (N) presented a Na content >1 atom nm^{-2} and Al_2O_3 (TH) < 0.005 atom nm^{-2} [37], so strong modification of the alumina acidic sites reflected in the catalytic activity in ethanol dehydration to ethylene, principal coke precursor. Raman spectra of the catalysts after SRA and SRE were registered (Fig. 2) in the 1200–1700 cm^{-1} region. All the spectra present two signals in 1320–1330 cm^{-1} and 1580–1590 cm^{-1} related to the defect mode, A_{1g} (signal D) and to the graphite mode, E_{2g} (signal G) respectively. The catalysts after SRA presented two weak signals and the catalysts after SRE presented two intense and asymmetrical, suggesting the superposition of carbon from different nature. The integrated intensity ratio of these two signals, D and G is related to the graphite crystallite size and it is possible to get the graphitic fraction, X_G (Table 2), according to [52]. Thereby, it is the catalyst Ni/Al_2O_3 (TH) the one which presents the highest X_G value (0.42) after SRE, indicating that the carbon is more structured and could impact the activity and stability of the catalyst. This is in agreement with the results from elemental analysis (C, wt%) and XRD after reaction and it can be deduced that the presence of both Rh and nanofibrous support can be related to the Ni particle size.

Steam reforming of acetone (SRA)

Acetone was selected as a model compound for the various carbonyl-containing (mainly aldehydes and ketones) constituents of the bio-oil. Fig. 3 shows the results in terms of mole fraction for Ni/Al_2O_3 (TH) and $Ni–Rh/Al_2O_3$(TH) catalysts during the SRA as function of temperature from 473 to 973 K. To evaluate the contribution of the thermal decomposition of acetone, the results for the homogeneous (non-catalytic) reaction was also examined and plotted considering the same reaction condition but packing the reactor with inert quartz particles of the same weight and particle size. For non-catalytic test (Fig. 3A) no activity was detected below 723 K.

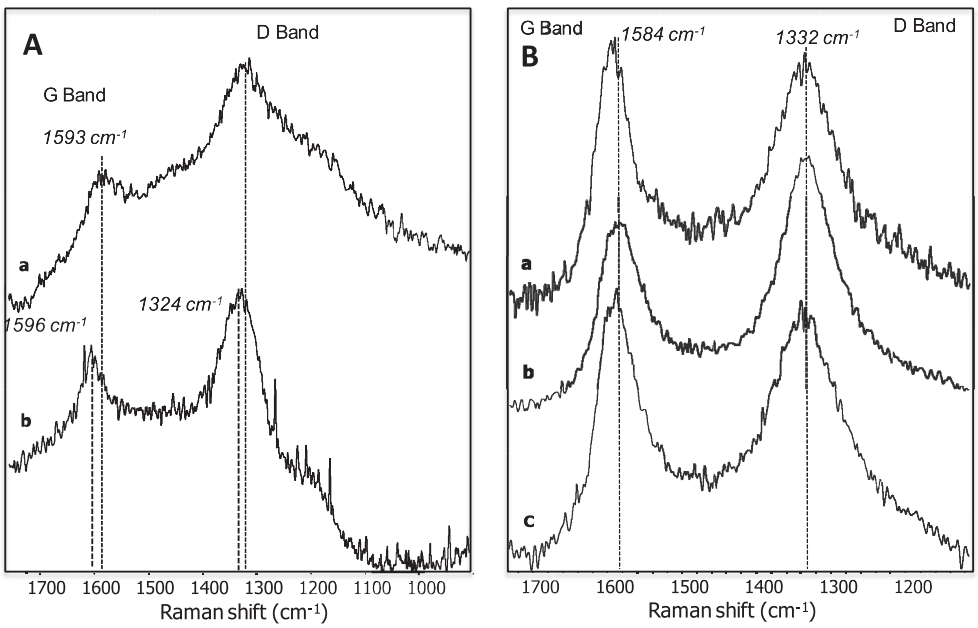

Fig. 2 – A. Raman spectra of the catalysts after SRA reaction. (a) Ni/Al_2O_3(TH); (b) $Ni–Rh/Al_2O_3$(TH). B. Raman spectra of the catalysts after SRE reaction (a) Ni/Al_2O_3(TH); (b) $Ni–Rh/Al_2O_3$(TH) and (c) Ni/Al_2O_3(N).

Please cite this article in press as: González-Gil R, et al., Production of hydrogen by catalytic steam reforming of oxygenated model compounds on Ni-modified supported catalysts. Simulation and experimental study, International Journal of Hydrogen Energy (2015), http://dx.doi.org/10.1016/j.ijhydene.2015.05.167

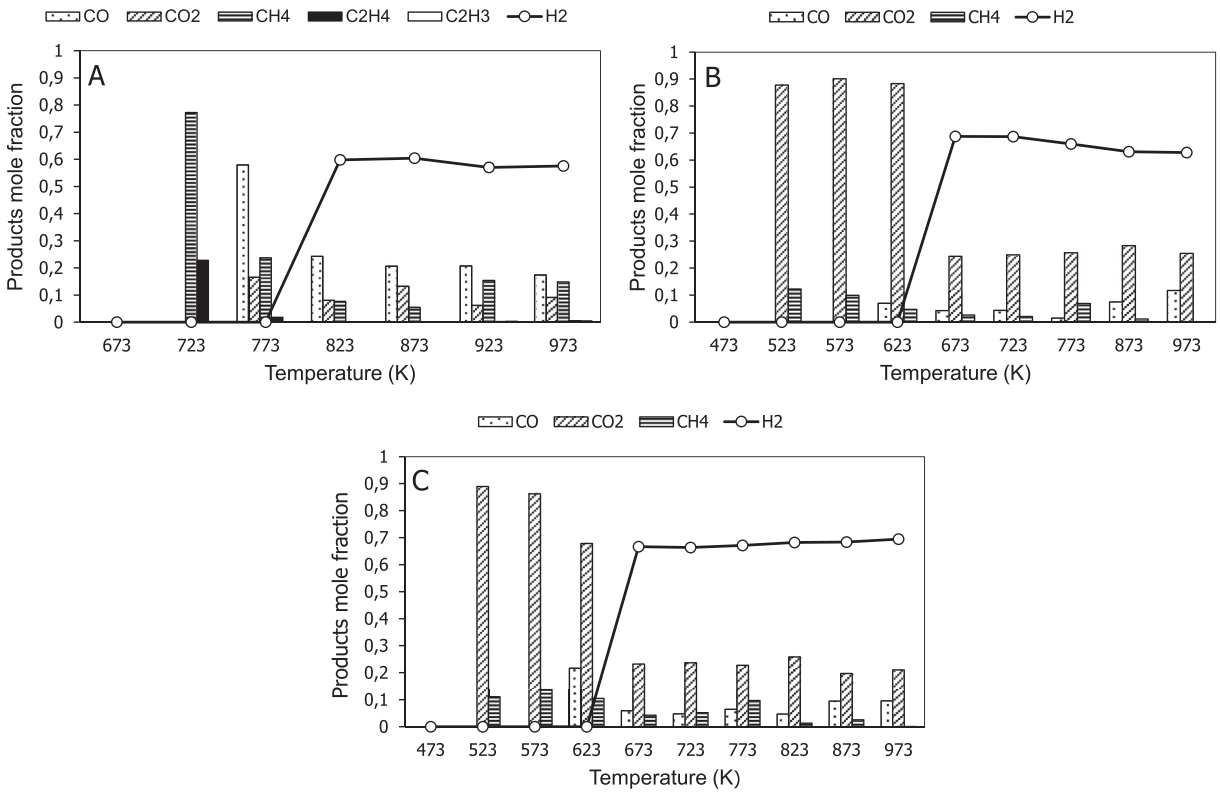

Fig. 3 – Steam reforming of acetone. Experimental conditions: gas flow rate acetone–water = 0.015 cm^3 min^{-1}, S/C = 3 diluted in He (30 ml min^{-1}), GHSV = 9000 h^{-1}. (A) Non-catalytic test. (B) Ni/Al_2O_3(TH) and (C) Ni–Rh/Al_2O_3(TH).

An acetone conversion value of 53% was registered at the maximum temperature studied (973 K). Methane and ethylene are the reaction products at low temperature (723 K). At 773 K besides CO as major product, CO_2 and CH_4 are also presents thought, at this temperature the production of H_2 is minimal. These results confirm that acetone is thermally decomposed under the conditions used in this study (Eqs. (7)–(8)) and are according to the results reported by Navarro et al. [53]. A high temperature (>823 K) is needed to obtain a maximum, and almost constant, H_2 selectivity value (0.6). The H_2/CO value was close to 3.3 at the highest temperature used and the H_2/CO_2 value around 7, a far higher value than the stoichiometric of Eq. (4) (2.7) indicates that acetone steam reforming (Eq. (4)) is not occurring under these conditions; registering a CO/CO_2 molar ratio >3.

Products distribution for SRA over Ni/Al_2O_3 (TH) catalyst is plotted in Fig. 3B. The conversion of acetone is 82% at the highest temperature, 973 K. H_2, CO, CO_2 and CH_4 are the only products detected. Maximum hydrogen mole fraction (0.69) is attained at 673 K, a much lower temperature than the needed for the non-catalytic test. An increase in the temperature is accompanied by a slight decrease in hydrogen concentration due probably to the Reverse Water Gas Shift (RWGS) reaction. In contrast to the non-catalytic experiment, CO_2 concentration is higher than CO in the whole range of temperatures considered, due to the occurrence of the acetone steam reforming reaction (Eq. (4)), registering a CO/CO_2 molar ratio < 1. The H_2/CO molar ratio achieved is 5, and a H_2/CO_2 value of 2.5, close to the stoichiometric value according to Eq. (4).

Fig. 3C plots the activity of the Ni–Rh/Al_2O_3(TH) in SRA. Total conversion of acetone was achieved and H_2, CO, CO_2 and CH_4 are the main products detected. In addition, traces of ethylene and ethane, and C_3 compound (0.08–0.14%), including the C_3-allene are also registered (not represented in the Figure). This is in agreement with the reported in the literature [34,53,54] except acetic acid, that is not detected in our tests. At 673 K a high decrease in the CO_2 production is denoted, due, possibly to the RWGS equilibrium. Methane mole fraction is relatively high at low temperatures, indicating that decomposition of acetone via Eq. (7), which is favored at temperatures over 750 K, occurs under these conditions. Ketene, also formed, may be converted via Eq. (8) to ethylene and CO [14], as even though in small amounts, ethylene was found in the products. In addition, at high temperature, the hydrogen mole fraction raised (0.7) much more than expected, due not only to acetone steam reforming but also to methane steam reforming. Additionally, steam reforming of ketene, a very unstable and reactive molecule, according to Eq. (12) is a possible reaction that can contribute to hydrogen concentration, as indicated in literature [14] since no ketene was found in the products. The H_2/CO molar ratio reached at 973 K is 7.3, higher than the value obtained with Ni/Al_2O_3 (TH), H_2/CO_2 valueis close to 3.3 at the maximum studied temperature. Rh role can be justified by the equilibrium between ethylene and ethane via hydrogenation. The small amount of the C_3-allene

Please cite this article in press as: González-Gil R, et al., Production of hydrogen by catalytic steam reforming of oxygenated model compounds on Ni-modified supported catalysts. Simulation and experimental study, International Journal of Hydrogen Energy (2015), http://dx.doi.org/10.1016/j.ijhydene.2015.05.167

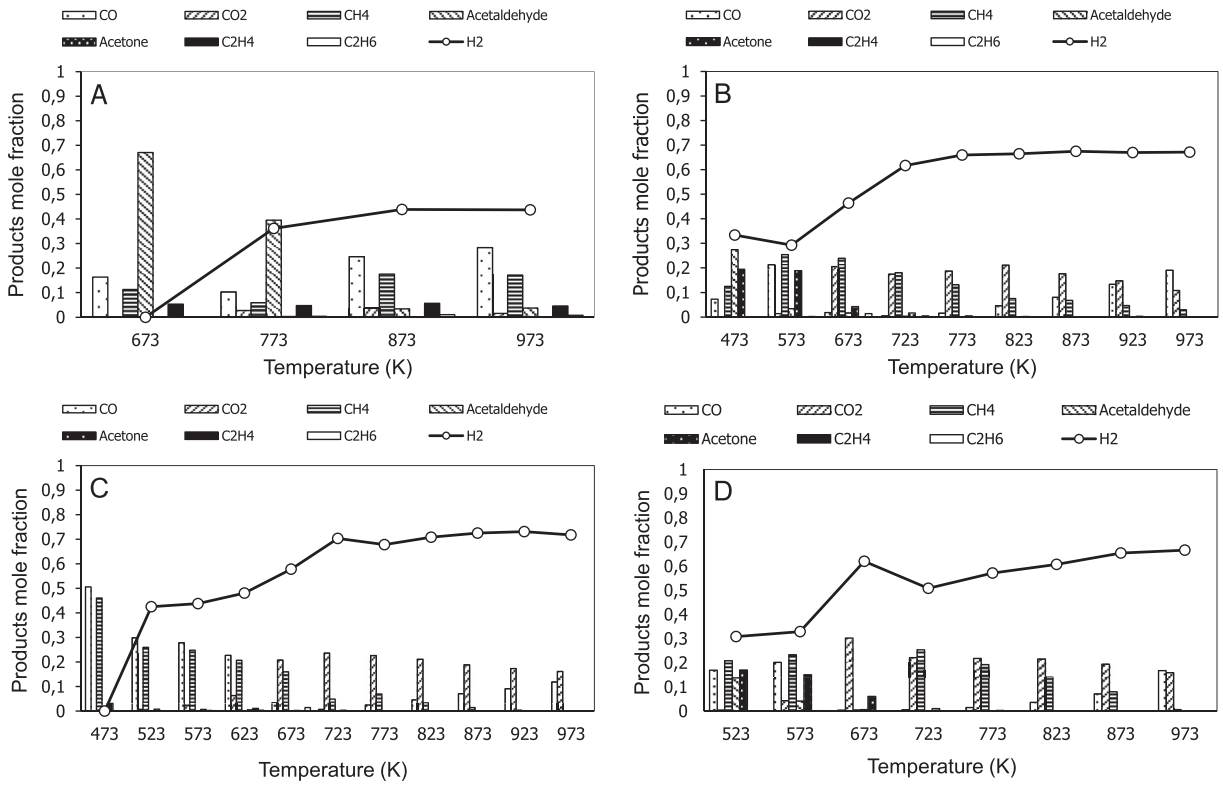

Fig. 4 – Steam reforming of ethanol. Experimental conditions: gas flow rate ethanol–water = 0.015 cm^3 min^{-1}; S/C = 2 diluted in He (30 ml min^{-1}), GHSV = 9000 h^{-1}. (A) Non-catalytic test. (B) Ni/Al_2O_3(TH). (C) Ni–Rh/Al_2O_3(TH) and (D) Ni/Al_2O_3(N).

detected in all temperature range is also justified by rhodium presence. These findings are in accordance with the reaction $2CH_2CO \leftrightarrow CH_2{=}C{=}CH_2 + CO_2$, contributing to raise the CO_2 selectivity. The incorporation of Rh to Ni modifies in different way the routes of formation of oligomer product observed on monometallic Ni catalyst.

Steam reforming of ethanol (SRE)

Ethanol was selected as part of the alcohols from bio oil and additionally, ethanol steam reforming is interesting by itself because it has been proposed as an alternative to fossil fuels. Fig. 4 depicts the results in terms of products mole fraction for Ni/Al_2O_3(TH), Ni–Rh/Al_2O_3(TH) and Ni/Al_2O_3(N) catalysts during the SRE as function of temperature from 473 to 973 K. Products distribution of the homogeneous (non-catalytic) reaction is also shown in Fig. 4A. No activity was observed below 673 K. The maximum ethanol conversion was 70% at the highest temperature studied. It is noticeable that for the whole range of temperatures under study, the products distribution corresponds to a series of reactions. The maximum H_2 content (0.43, expressed in mole fraction) is registered at 873 K. For further temperature increases, the intermediate products obtained are, mostly, acetaldehyde and ethylene coming from ethanol dehydrogenation (Eq. (14)) and dehydration (Eq. (16)) reactions. Furthermore, CH_4, CO and H_2 are obtained as a result of acetaldehyde decarboxylation and ethanol decomposition. The effect of water gas shift (Eq. (2)) and methane steam reforming (SRM) (Eqs. (19) and (20)) reactions is insignificant, as low CO_2 and high CH_4 amounts are detected. Moreover, CH_4, CO and H_2 mole fractions remain constant at temperatures >800 K.

Fig. 4B shows the products distribution obtained for the SRE process with the Ni/Al_2O_3 (TH) catalyst. An ethanol conversion of 90% was reached. As it can be observed, at low temperatures (<673 K), the main products are acetone (C_3H_6O), acetaldehyde (C_2H_4O) and ethylene (C_2H_4), which is consistent to the reported in literature [26]. These intermediates are due to ethanol decomposition/oligomerization (Eq. (18)), ethanol dehydrogenation (Eq. (14)) and ethanol dehydration (Eq. (16)) reactions, respectively. 0.60 of H_2 mole fraction is registered at 723 K which is maintained when temperature increases. Final products such as CH_4, H_2 and CO were also observed due to the ethanol direct decomposition. With regard to the intermediates, the amount of acetone observed is significant, (0.20) whilst acetaldehyde and ethylene is lower than 0.05. Zhang et al. [55] agree that acetone and acetaldehyde are the main intermediates observed below 700 K. Therefore these results imply that for the temperature range between 473 and 673 K the process goes mainly though ethanol decomposition and subsequent oligomerization to acetone (Eq. (18)). In addition, for the temperature range between 673 and 773 K, the occurrence of the WGS and SRM reactions was denoted due to the increase of the H_2 and CO_2 production and the

Please cite this article in press as: González-Gil R, et al., Production of hydrogen by catalytic steam reforming of oxygenated model compounds on Ni-modified supported catalysts. Simulation and experimental study, International Journal of Hydrogen Energy (2015), http://dx.doi.org/10.1016/j.ijhydene.2015.05.167

decrease for CH_4 and CO. However, above 773 K the occurrence of the SRM reactions causes the decrease in the CH_4 content and the subsequent increases in the H_2 and CO_2 production. Moreover, the RWGS reaction causes, again, an increase in the CO selectivity in detriment of the H_2 and CO_2. Above 800 K, the opposite effect of the SMR and RWGS reactions causes a constant H_2 and CO_2 production whilst CO selectivity increases, which implies that the SRM reaction occurs mainly through reforming of methane to CO_2 with two molecules of water.

Products distribution obtained with the Ni–Rh/Al_2O_3 (TH) catalyst is given in Fig. 4C. 80% of ethanol conversion was reached. At low temperatures (<600 K), in comparison with the Ni/Al_2O_3(TH) monometallic catalysts, it is noticeable that the presence of intermediates is negligible. Secondary reactions such as dehydration, dehydrogenation and decomposition reactions towards acetaldehyde, ethylene and acetone, respectively, are restricted and only the ethanol decomposition to CH_4, CO and H_2 is significant. With the increase of temperature, the products distribution reflects the same trend as before due to the occurrence of the SMR, WGS and RWGS reactions. Moreover, the addition of Rh, as observed reduces the temperature where maximum H_2 selectivity is obtained and increases its value, reaching a mole fraction of 0.7 at 723 K.

Products distribution obtained with the Ni/Al_2O_3 (N) catalyst are shown in Fig. 2D. In comparison with the monometallic TH-alumina supported catalyst, non-significant differences were obtained in the products distribution. Hydrogen production reaches, in both cases, values around 0.6–0.7 for temperatures above 800 K, which is consistent with other results found in literature for the SRE process [51,56]. Nevertheless, it is worth pointing out that the absence of ethylene with this catalyst is influenced by the nature of the support and mainly by the acidic properties. As can be found in Ref. [37] the Na content in the nanofibrous support implies weaker OH's acidity in comparison with the commercial TH-alumina support, which means lower selectivity towards ethylene formation, which is the main precursor of carbon formation and, therefore, catalyst deactivation.

Mathematical modeling results of SRA and SRE. Study of operating conditions

Steam reforming of the model compounds, a mixture of acetone/water or ethanol/water, was simulated in a temperature range of 773 and 1300 K in acetone steam reforming and between 473 and 1173 K for ethanol steam reforming, in order to study the process behavior. The effect of S/Acetone or S/Ethanol feed molar ratios and temperature over acetone/ethanol conversion and over H_2/CO ratio was presented in 3D diagrams, for different space velocities, aiming to found the regions and the optimal operating conditions in both processes.

Fig. 5 shows the simulation results of SRA taking into account the reaction and the kinetics parameters in Table 1. The effect of feed molar ratio and temperature on acetone conversion is plotted in Fig. 5A and on the H_2/CO is presented in Fig. 5B. SRA simulation was studied between 773 and 1273 K and using three inlet molar flows of acetone: 0.004 mol h^{-1} (which was used in the experimental test of SRA), 0.1 and 1 mol h^{-1}. For 0.004 mol h^{-1} and 0.1 mol h^{-1}, a complete acetone conversion is predicted for the whole temperature range and feedstock ratio used. Though, when the acetone molar inlet flow is 1 mol h^{-1} a 60% of conversion was reached at low temperature and S/Acetone = 1. H_2/CO ratio is further influenced by space velocity, finding different surfaces depending also on the molar flow. Using a space velocity of 1 mol h^{-1} of acetone, a plane surface is found with an approximately constant H_2/CO value below 0.5. A decrease in acetone feedstock, 0.1 mol h^{-1}, is accompanied by a quite difference in the surface obtained, achieving a maximum local value of H_2/CO close to 1.5 at 1273 K and S/Acetone = 1. At lower temperature and higher steam to acetone ratio used, the surface decrease to a value of 0.5. The maximum hydrogen content is found with experimental data at S/Acetone between 2 and 3. On the other hand, it was found that the H_2/CO

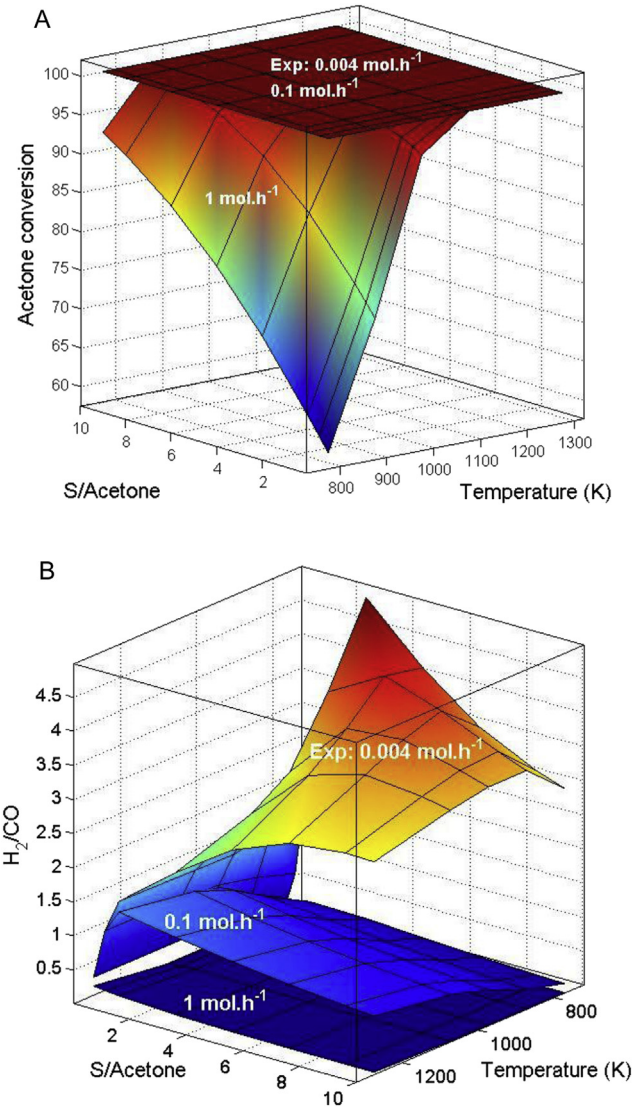

Fig. 5 – Mathematical modeling results for Steam Reforming of Acetone (SRA). Effect of temperature and steam/acetone (S/A) on (A) acetone conversion and (B) H_2/CO molar ratio for three inlet flow of acetone.

Please cite this article in press as: González-Gil R, et al., Production of hydrogen by catalytic steam reforming of oxygenated model compounds on Ni-modified supported catalysts. Simulation and experimental study, International Journal of Hydrogen Energy (2015), http://dx.doi.org/10.1016/j.ijhydene.2015.05.167

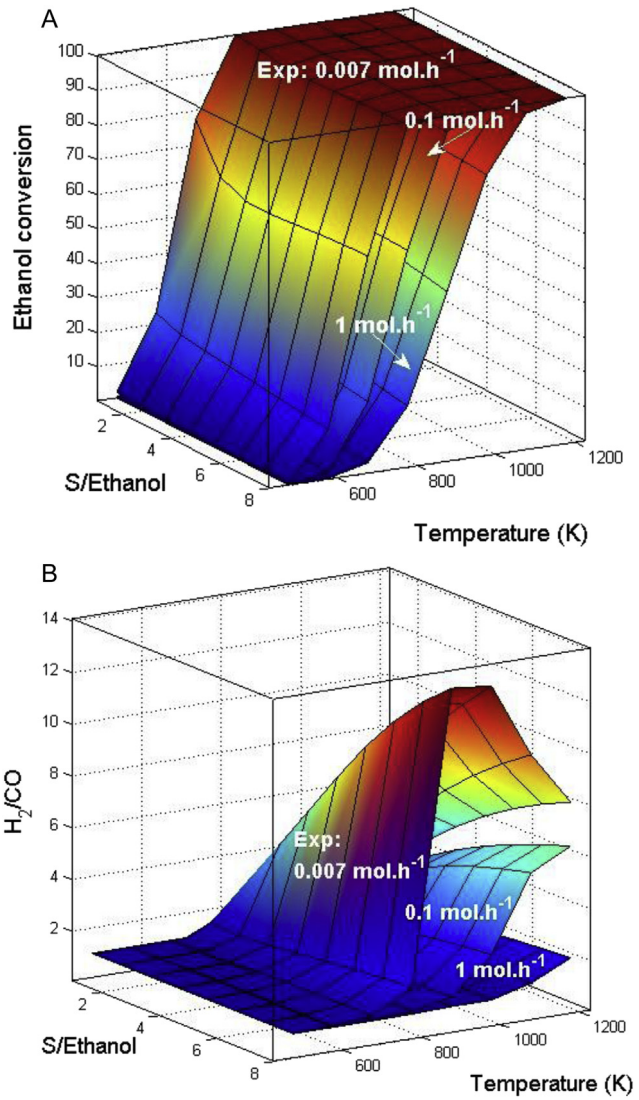

Fig. 6 – Mathematical modeling results for Steam Reforming of Ethanol (SRE). Effect of temperature and steam/ethanol (S/E) molar ratio on (A) ethanol conversion and (B) H_2/CO molar ratio for three inlet flow of ethanol.

ratio is particularly dependent on temperature. The H_2/CO ratio produced was increased by increasing the temperature but in experimental conditions, a maximum value close to 4.7 was found between 773 and 873 K and S/Acetone between 2 and 3. The composition of inlet feedstock is an important parameter to consider, so as steam is a co-reactant, and agreeing with S/Acetone effect studied, a steam to acetone ratio over 5 promotes steam reaction with high hydrogen yield. According to 3D diagram and in agreement with our experimental results, an S/Acetone ratio close to 9 (equivalent to S/C = 3, optimum ratio to reduce coke formation) satisfies criteria for high hydrogen concentration and for syngas composition, using a reactor temperature of 973 K.

According to the reactions network and the kinetics parameters proposed in Table 1, results from the mathematical model simulation of steam reforming of ethanol (SRE) in function of temperature (473–1173 K) and S/Ethanol ratios, for three inlet flow of ethanol: 0.007 mol h^{-1} (which was used in the experimental tests of SRE), 0.1 and 1 mol h^{-1}, are shown in Fig. 6. Ethanol conversion curves are plotted in Fig. 6A and H_2/CO ratio in Fig. 6B. It is noticeable that an increase of ethanol in the feed (low S/Ethanol) is accompanied by a shift of the response curves towards lower conversions, which means that to guarantee a total ethanol conversion, high temperatures are needed. López et al. [51] studied the effect of the feed composition, steam to carbon molar ratio, using structured catalysts. This parameter could affect the ethanol conversion according to the operating temperature through equilibrium limitations and dilution effects. However, due to the large value of the ethanol fed considered here for fixed-bed catalyst, which is higher than those typically used for structured catalysts, the feed composition S/Ethanol does not present a significant effect on the ethanol conversion. As observed, total ethanol conversion is achieved above 700, 900 and 1100 K for 0.007, 0.1 and 1 mol h^{-1}respectively. Thus, the ethanol fed, expressed here as the ethanol feed flow rate, has influence on the ethanol conversion, regardless of the S/Ethanol ratio. Nevertheless, the steam to ethanol molar ratio and temperature have a significant effect on the H_2/CO ratio. The H_2/CO molar ratio increases with temperature and S/Ethanol ratio until a maximum value close to 13.4 at S/Ethanol = 8 and 873 K. When the ethanol feed flow rate is incremented in one and two orders of magnitude (0.1 and 1 mol h^{-1}), the H_2/CO maximum value decreases and is reached at the higher temperature studied (6.5 and 2.2 at 1173 K and S/Ethanol = 8 for ethanol feed of 0.1 and 1 mol h^{-1} respectively). As mentioned before, the increase in the ethanol feed is related to lower reaction periods, lower ethanol conversion and, therefore, lower H_2/CO ratio. It can be observed that the feed composition plays an important role in regard to the selectivity of H_2/CO due to the fact that an increase in the partial pressure of H_2O in the feed implies a displacement of the equilibrium of the SRM and WGS reactions (Eqs. (19), (20) and (2), respectively) towards a higher H_2 production in detriment of a lower CO production. Besides, it is noticeable that a higher content of H_2O in the feed entails that the SRM occurs principally through steam reforming towards CO_2 with two molecules of water rather than to CO with one molecule of water. This effect is not significant at higher temperatures where both SRM reactions are promoted.

Conclusions

Acetone and ethanol can be efficiently reformed to a hydrogen rich stream over the catalysts used, with H_2 production between 0.6 and 0.7 (expressed as mole fraction) above 800 K. Different reforming routes were observed. H_2, CO, CO_2 and CH_4 are the major products detected for Ni/Al_2O_3(TH) and Ni–Rh/Al_2O_3(TH) in the SRA and SRE. Besides steam reforming of acetone, reverse water gas shift and steam reforming of methane occurs. Rh also play an important role in the SRA since it allows full acetone conversion promoting H_2 production with minimal carbon deposition after catalytic test. Ethanol reforming occurs mainly via ethanol decomposition to acetone, acetaldehyde and ethylene followed by steam

Please cite this article in press as: González-Gil R, et al., Production of hydrogen by catalytic steam reforming of oxygenated model compounds on Ni-modified supported catalysts. Simulation and experimental study, International Journal of Hydrogen Energy (2015), http://dx.doi.org/10.1016/j.ijhydene.2015.05.167

reforming and decomposition of these intermediates. Rh incorporation, even in minimal loading 1:100 (Rh:Ni) diminish the intermediate products promoting the ethanol decomposition reaction. The effect of the alumina is understood in base to its acidity, since no ethylene was found with $Ni/Al_2O_3(N)$ and the carbon content after reaction is significantly reduced. Matlab modeling permitted to find out the optimal operating regions and predict the experimental data obtained.

Acknowledgments

The authors want to acknowledge to the Spanish Ministry of Economy and Competitiveness the Financial support of PRI-PIBAR 2011-1343.

REFERENCES

[1] Kuhn JN, Zhao Z, Felix LG, Slimane RB, Choi CW, Ozkan US. Olivine catalysts for methane and tar- steam reforming. Appl Catal B Environ 2008;81:14–26.
[2] Faroldi BM, Lombardo EA, Cornaglia LM, Irusta S. Application of ETS-10 microporous titanosilicate as support of Ru nanoparticles for hydrogen production. Appl Catal A Gen 2012;417–418:43–52.
[3] Bradford MCJ, Vannice MA. CO_2 reforming of CH_4. Catal Rev Sci Eng 1999;41(1):1–42.
[4] Rostrup-Nielsen JR, Sehested J. Hydrogen and synthesis gas by steam and CO_2 reforming. Adv Catal 2002;47:65–139.
[5] Hoang DL, Chan SH, Ding OL. Kinetic and modelling study of methane steam reforming over sulfide nickel catalyst on a gamma alumina support. Chem Eng J 2005;112:1–11.
[6] Sá S, Silva H, Brandão L, Sousa JM, Mendes A. Catalysts for methanol steam reforming. A review. Appl Catal B Environ 2010;99:43–57.
[7] García-Diéguez M, Pieta IS, Herrera MC, Larrubia MA, Alemany LJ. Improved Pt-Ni nanocatalysts for dry reforming of methane. Appl Catal A: Gen 2010;377:191–9.
[8] García-Diéguez M, Pieta IS, Herrera MC, Larrubia MA, Alemany LJ. Nanostructured Pt- and Ni-based catalysts for CO_2-reforming of methane. J Catal 2010;270:136–45.
[9] García-Diéguez M, Pieta IS, Herrera MC, Larrubia MA, Alemany LJ. Rh-Ni nanocatalysts for the CO_2 and CO_2+H_2O reforming of methane. Catal Today 2011;172:136–42.
[10] Parthasarathy P, Sheeba Narayanan K. Hydrogen production from steam gasification of biomass: influence of process parameters on hydrogen yield. A review. Renew Energy 2014;66:570–9.
[11] Díaz-Rey MR, Cortés-Reyes M, Herrera C, Larrubia MA, Amadeo N, Laborde M, et al. Hydrogen-rich gas production from algae-biomass by low temperature catalytic gasification. Catal Today 2014. http://dx.doi.org/10.1016/j.cattod.2014.04.035.
[12] Hu X, Lu G. Bio-oil steam reforming, partial oxidation or oxidative steam reforming coupled with bio-oil dry reforming to eliminate CO_2 emission. Int J Hydrog Energy 2010;35:7169–76.
[13] Remón J, Broust F, Valette J, Chhiti Y, Alava I, Fernandez-Akarregi AR, et al. Production of a hydrogen-rich gas from fast pyrolysis bio-oils: comparison between homogeneous and catalytic steam reforming routes. Int J Hydrog Energy 2014;39:171–82.
[14] Trane R, Dahl S, Skøth-Rasmnussen MS, Jensen AD. Catalytic steam reforming of bio-oil. Int J Hydrog Energy 2012;37:6447–72.
[15] Bertero M, de la Puente G, Sedran U. Fuels from bio-oils: bio-oil production from different residual sources, characterization and thermal conditioning. Fuel 2012;95:263–71.
[16] Kechagiopoulos PN, Voutetakis SS, Lemonidou AA, Vasalos IA. Sustainable hydrogen production via reforming of ethylene glycol using a novel spouted bed reactor. Catal Today 2007;127:246–55.
[17] Kechagiopoulos PN, Voutetakis SS, Lemonidou AA, Vasalos IA. Hydrogen production via steam reforming of the aqueous phase of bio-oil in a fixed bed reactor. Energy & Fuel 2006;20:2155–63.
[18] Xie J, Su D, Yin X, Wu C, Zhu J. Thermodynamic analysis of aqueous phase reforming of three model compounds in bio-oil for hydrogen production. Int J Hydrog Energy 2011;36:15561–72.
[19] Resini C, Arrighi L, Herrera Delgado MC, Larrubia Vargas MA, Alemany LJ, Riani P, et al. Production of hydrogen by steam reforming of C_3 organics over Pd-Cu/α-Al_2O_3 catalyst. Int J Hydrog Energy 2006;31:13–9.
[20] Nogueira FGE, Assaf PGM, Carvalho HWP, Assaf EM. Catalytic steam reforming of acetic acid as a model compound of bio-oil. Appl Catal B Environ 2014;160–161:188–99.
[21] Latifi M, Berruti F, Briens C. Non-catalytic and catalytic steam reforming of a bio-oil model compound in a novel "Jiggle Bed" reactor. Fuel 2014;129:278–91.
[22] Hu X, Lu G. Investigation of steam reforming of acetic acid to hydrogen over Ni-Co metal catalyst. J Mol Catal A Chem 2007;261:43–8.
[23] Bimbela F, Oliva M, Ruiz J, García L, Arauzo J. Hydrogen production by catalytic steam reforming of acetic acid, a model compound of biomass pyrolysis liquids. J Anal Appl Pyrolysis 2007;79:112–20.
[24] Takanabe K, Aika K, Seshan K, Lefferts L. Catalyst deactivation during steam reforming of acetic acid over Pt/ZrO_2. Chem Eng J 2006;120:133–7.
[25] Vaidya PD, Rodrigues AE. Insight into steam reforming of ethanol to produce hydrogen for fuel cells. Chem Eng J 2006;117:39–49.
[26] Benito M, Sanz JL, Isabel R, Padilla R, Arjona R, Daza L. Bio-ethanol steam reforming: Insights on the mechanism for hydrogen production. J Power Sources 2005;151:11–7.
[27] Vicente J, Ereña J, Montero C, Azkoiti MJ, Bilbao J, Gayubo AG. Reaction pathway for ethanol steam reforming on a Ni/SiO_2 catalyst including coke formation. Int J Hydrog Energy 2014;39:18820–34.
[28] Barattini L, Ramis G, Resini C, Busca G, Sisani M, Constantino U. Reaction path of ethanol and acetic acid steam reforming over Ni-Zn-Al catalysts. Flow reactor studies. Chem Eng J 2009;153:43–9.
[29] Li Z, Hu X, Zhang L, Liu S, Lu G. Steam reforming of acetic acid over Ni/ZrO_2 catalysts: effects of nickel loading and particle size on product distribution and coke formation. Appl Catal A Gen 2012;417–418:281–9.
[30] Hu X, Lu G. Acetic acid steam reforming to hydrogen over Co-Ce/Al_2O_3 and Co-La/Al_2O_3 catalysts. The promotion effect of Ce and La addition. Catal Commun 2010;2:50–3.
[31] Matas Güel B, Babich I, Nichols KP, Gardeniers JGE, Seshan K. Design of a stable steam reforming catalyst. A promising route to sustainable hydrogen from biomass oxygenates. Appl Catal B Environ 2009;90:38–44.
[32] Iriondo A, Barrio VL, Cambra JF, Arias PL, Güemez MB, Navarro RM, et al. Influence of La_2O_3 modified support and Ni and Pt active phases on glycerol steam reforming to produce hydrogen. Catal Commun 2009;10:1275–8.

Please cite this article in press as: González-Gil R, et al., Production of hydrogen by catalytic steam reforming of oxygenated model compounds on Ni-modified supported catalysts. Simulation and experimental study, International Journal of Hydrogen Energy (2015), http://dx.doi.org/10.1016/j.ijhydene.2015.05.167

[33] Bettman M, Chase RE, Otto K, Weber WH. Dispersion studies on the system La_2O_3/α-$_2O_3$. J Catal 1989;117:447–54.
[34] Rioche C, Kulkarni S, Meunier FC, Breen JP, Burch R. Steam reforming of model compounds and fast pyrolysis bio-oil on supported metal catalysts. Appl Catal B Environ 2005;61:130–9.
[35] Liguras DK, Kondarides DI, Verykios XE. Production of hydrogen for fuel cells by steam reforming of ethanol over supported noble metal catalysts. Appl Catal B Environ 2003;43:345–54.
[36] García-Diéguez M, Herrera C, Larrubia MA, Alemany LJ. CO_2-reforming of natural gas components over a highly stable and selective NiMg/Al_2O_3 nanocatalyst. Catal Today 2012;197:50–7.
[37] Phung TK, Herrera C, Larrubia MA, García-Diéguez M, Finocchio E, Alemany LJ, et al. Surface and catalytic properties of some γ-Al_2O_3 powders. Appl Catal A General 2014;483:41–51.
[38] Vagia EC, Lemonidou AA. Thermodynamic analysis of hydrogen production via steam reforming of selected components of aqueous bio-oil fraction. Int J Hydrog Energy 2007;32:212–23.
[39] da Silva AL, Malfatti CF, Müller IL. Thermodynamic analysis of ethanol steam reforming using Gibbs energy minimization method: a detailed study of the conditions of carbon deposition. Int J Hydrog Energy 2009;34:4321–30.
[40] Froment G, Pijcke H, Goethals G. Thermal cracking of acetone – I. Chem Eng Sci 1961;13:173–9.
[41] Sato K, Hidaka Y. Shock-Tube modeling study of acetone pyrolysis and oxidation. Combust Flame 2000;122:291–311.
[42] Harris PS, Baker RTK, Birch RA. The formation of carbon deposits from decomposition of acetone over nickel. Carbon 1973;11:531–9.
[43] Lam K, Ren W, Pyun SH, Farooq A, Davidson DF, Hanson RK. Multi-species time-history measurements during high-temperature acetone and 2-butanone pyrolysis. Proc Combust Inst 2013;34:607–15.
[44] Tsuda M, Kuratan K. Thermal decomposition of ketene in shock waves. Bull Chem Soc Jpn 1698;41:53–60.
[45] Youn MH, Seo JG, Lee H, Bang Y, Chung JS, Song IK. Hydrogen production by auto thermal reforming of ethanol over nickel catalysts supported on metal oxides: effect of support acidity. Appl Catal B Environ 2010;98:57–64.
[46] Seker E. The catalytic reforming of bio-ethanol over SiO_2 supported ZnO catalysts: the role of ZnO loading and the steam reforming of acetaldehyde. Int J Hydrog Energy 2008;33:22044–52.
[47] Elias KFM, Lucrédio AF, Assaf EM. Effect of CaO addition on acid properties of Ni-Ca/Al2O3 catalysts applied to ethanol steam reforming. Int J Hydrog Energy 2013;38:4407–17.
[48] Phung TK, Lagazzo A, Rivero Crespo MA, Ecribano VS, Busca G. A study of commercial transition aluminas and of their catalytic activity in the dehydration of ethanol. J Catal 2014;311:102–13.
[49] Choong CKS, Huang L, Zhong Z, Lin J, Hong L, Chen L. Effect of calcium addition on catalytic ethanol steam reforming of Ni/Al_2O_3: II. Acidity/basicity, water adsorption and catalytic activity. Appl Catal A Gen 2011;407:155–62.
[50] Nishiguchi T, Matsumoto T, Kanai H, Utani K, Matsumura Y, Shen W, et al. Catalytic steam reforming of ethanol to produced hydrogen and acetone. Appl Catal A Gen 2005;279:273–7.
[51] López E, Divins NJ, Anzola A, Schbib S, Borio D, Llorca J. Ethanol steam reforming for hydrogen generation over structured catalysts. Int J Hydrog Energy 2013;38:4418–28.
[52] Ulla MA, Valera A, Ubieto T, Latorre N, Romeo E, Milt VG, et al. Carbon nanofiber growth onto a cordierite monolith coated with co-mordenite. Catal Today 2008;133:7–12.
[53] Navarro RM, Guil-Lopez R, González-Carballo JM, Cubero A, Ismail AA, Al-Sayari SA, et al. Bimetallic MNi/Al_2O_3-La catalysts (M=Pt, Cu) for acetone steam reforming: role of M on catalyst structure and activity. Appl Catal A Gen 2014;474:168–77.
[54] ECh Vagia, Lemonidou AA. Hydrogen production via steam reforming of bio-oil components over calcium aluminate supported nickel and noble metal catalysts. Appl Catal A Gen 2008;351:111–21.
[55] Zhang B, Tang X, Li Y, Cai W, Xu Y, Shen W. Steam reforming of bio-ethanol over ceria-supported Co, Ir and Ni catalysts. Catal Commun 2006;7:367–72.
[56] Llera I, Mas V, Bergamini ML, Laborde M, Amadeo N. Bio-ethanol steam reforming on Ni based catalyst. Kinetic study. Chem Eng Sci 2012;71:356–66.

Please cite this article in press as: González-Gil R, et al., Production of hydrogen by catalytic steam reforming of oxygenated model compounds on Ni-modified supported catalysts. Simulation and experimental study, International Journal of Hydrogen Energy (2015), http://dx.doi.org/10.1016/j.ijhydene.2015.05.167